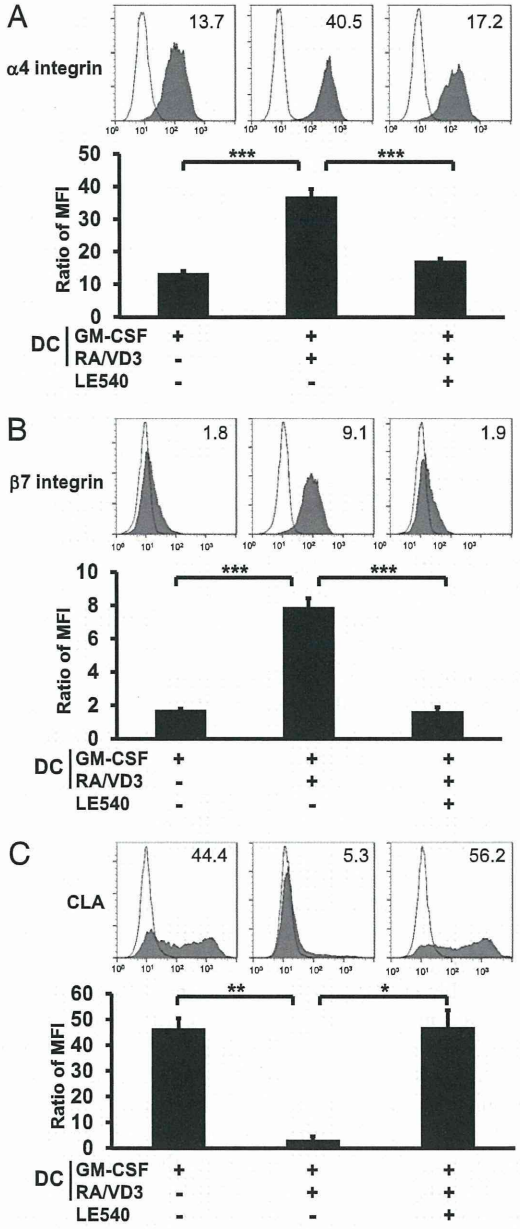

FIGURE 5. RALDH2^{high} mDCs induce gut-homing and suppress skin-homing molecules on CD4$^+$ T cells in an RA-dependent manner. CD1c$^+$ mDCs were cultured with GM-CSF alone (RALDH2^{low} mDCs) or GM-CSF, RA, and VD_3 (RALDH2^{high} mDCs) for 2 d. The DCs were collected and extensively washed. Then allogeneic naive CD4$^+$ T cells were stimulated with RALDH2^{low} mDCs or RALDH2^{high} mDCs in the absence or presence of LE540 for 6 d. The T cells were stained for α_4 integrin (**A**), β_7 integrin (**B**), or CLA (**C**). Open histograms represent cells stained with isotype-matched control mAbs. The numbers shown with each histogram represent ratios of mean fluorescence intensity (MFI) of each surface molecule to that of isotype-matched control. The histograms are representative data, and the graphs show the mean ± SE from six (A, B) or three (C) independent experiments. $*p < 0.05$, $**p < 0.01$, $***p < 0.001$.

the immune system in humans, that is, a "vitamin D – CD1c$^+$ mDC – RA" axis for immune regulation.

Which DCs produce RA will be determined by two factors: 1) environmental signals DCs receive, and 2) intrinsic nature of each DC subset. In mice, RA (4–8), GM-CSF (4), IL-4 (4, 9), and TLR ligands (2, 4, 5, 10–12) induce DCs to express RALDH2. In humans, RA (5), Pam_3CSK_4 (5, 12), and a peroxisome proliferator–activated receptor γ ligand (rosiglitazone) (31) augment the expression of RALDH2 in MoDCs. In this study, to our knowledge, we demonstrated for the first time that VD_3 induces CD1c$^+$ mDCs to express a high level of RALDH2 in the presence of GM-CSF. Whereas exogenous RA moderately augmented the induction, neither IL-4 nor various immunomodulatory reagents including rosiglitazone augmented it. Notably, proinflammatory factors, TLR ligands and TNF, strongly suppressed ALDH activity. These data suggest that VD_3 is a key factor to induce human CD1c$^+$ mDCs to express RALDH2 in the steady state.

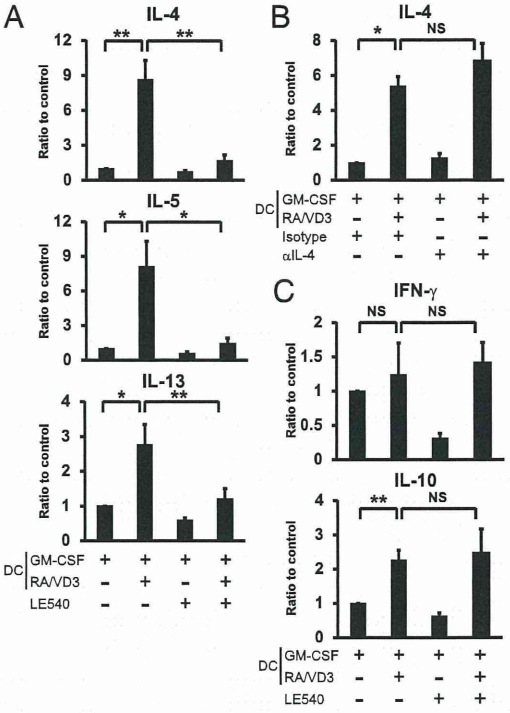

FIGURE 6. RALDH2^{high} mDCs induce CD4$^+$ T cells to produce Th2 cytokines in an RA-dependent manner. CD1c$^+$ mDCs were cultured as in Fig. 5 and were collected and extensively washed. Then allogeneic naive CD4$^+$ T cells were cocultured with RALDH2^{low} mDCs or RALDH2^{high} mDCs in the absence or presence of LE540 for 6 d (**A**, **C**) or in the presence of rat IgG1 (isotype) or anti–IL-4 mAb (**B**). The stimulated T cells were restimulated for 24 h, and the supernatants were analyzed for cytokines by ELISA. The data are normalized to the value obtained from CD4$^+$ T cells cocultured with RALDH2^{low} mDCs in the absence of LE540 or anti–IL-4 mAb. The data are shown as the mean ± SE of eight (A, C) or three (B) independent experiments. $*p < 0.05$, $**p < 0.01$. The mean and ranges of absolute cytokine concentrations from T cells cocultured with RALDH2^{low} mDCs in the absence of LE540 or anti–IL-4 mAb were as follows: (A) IL-4, 79.5 pg/ml (46.8–145 pg/ml); IL-5, 57.9 pg/ml (15.6–122 pg/ml); IL-13, 1720 pg/ml (321–4547 pg/ml); (B) IL-4, 63.9 pg/ml (42.9–104 pg/ml); and (C) IFN-γ, 28.5 ng/ml (9.48–80.6 ng/ml), and IL-10, 219 pg/ml (93.6–416 pg/ml).

It has been shown that VD_3 inhibits the expression of RALDH2 in mouse DCs (32). In addition, VD_3 represses RA-transcriptional activity via VDR in human myeloid cells (33). These findings indicate that VD_3 antagonizes the activity of RA. Thus, the cooperation between exogenous VD_3 and endogenously induced RA for the induction of RALDH2 in human CD1c$^+$ mDCs was unexpected. These results indicate that signaling pathways triggered by RA and VD_3 may antagonize or synergize, depending on cell types, coexisting factors, and/or species.

Among the human DC subsets we examined, CD1c$^+$ mDCs was the only subset that expresses a high level of RALDH2 in response to VD_3. Human CD141^{high} mDCs and their equivalent, mouse CD8$^+$CD11b$^-$ cDCs in lymphoid tissues (18) and CD103$^+$ cDC in

nonlymphoid tissues (17), share capacities to efficiently cross-present Ags to $CD8^+$ T cells (14–17). In contrast, distinctive functions of $CD1c^+$ mDCs, an equivalent of mouse $CD8^-CD11b^+$ cDCs (18), have been elusive. The present study suggests that, in contrast to $CD141^{high}$ mDCs, $CD1c^+$ mDCs may function as immunoregulatory DCs by preferentially producing RA upon exposure to VD_3.

Although several studies have shown that human MoDCs express RALDH2 (5, 12, 19, 31), gene expression profiling has shown that MoDCs markedly differ from the three subsets of human DCs in blood and lymphoid tissues and are more similar to macrophages (18). In addition, it remains to be determined to what extent monocytes differentiate into DCs in vivo in humans. Thus, the RALDH2 expression in $CD1c^+$ mDCs is likely to be more relevant to DC biology in vivo than that in MoDCs. Intriguingly, monocytes but not MoDCs exhibited a substantial level of ALDH activity in response to GM-CSF, RA, and VD_3, suggesting that $CD1c^+$ mDCs and monocytes may have similar machinery to express RALDH2.

Whereas freshly isolated mouse intestinal $CD103^+$ DCs but not $CD103^-$ DCs produce RA (3), we showed that 1) freshly isolated human MLN DCs do not have ALDH activity and that 2) $CD103^-$ mDCs but not $CD103^+$ mDCs in MLNs gain a high level of ALDH activity in response to the VD_3-containing stimulus. Although our data does not clarify the relationship between mouse and human DC subsets in MLNs, the data suggest that CD103 may not be a marker of DCs that preferentially produce RA in human MLNs. Jaesson et al. (34) reported that $CD103^+$ DCs from human MLNs induce T cells to express $\alpha_4\beta_7$ integrin and CCR9 in an RAR signaling–dependent manner. However, such DCs neither exhibited ALDH activity (Fig. 2A, 2B) nor induced T cells to express these gut-homing molecules (data not shown) in our experiments. Because Jaesson et al. (34) did not directly examine ALDH activity of MLN DCs, the reason for the discrepancy between the two studies is not clear.

Furthermore, GM-CSF alone was sufficient to induce high levels of ALDH activity in both of the cDC subsets in mouse spleen ($CD8^+$ and $CD8^-$) and MLNs ($CD103^+$ and $CD103^-$), and VD_3 did not augment the activity. Thus, DC subsets capable of acquiring ALDH activity and the stimulation to induce DCs to acquire the activity appear to be significantly different between humans and mice.

RA (5) or zymosan (11) induces mouse splenic DCs to express RALDH2 through RAR or TLR2, respectively, in an ERK-dependent manner. Pam_3CSK_4 induces mouse splenic DCs to express RALDH2 in a JNK-dependent manner (12). In contrast, we showed that p38 but not MEK or JNK is necessary to induce human $CD1c^+$ mDCs to express RALDH2 in response to VD_3. Thus, although MAPK is important for the induction of RALDH2 in DCs, it appears that which MAPK is involved depends on the type of stimuli and/or species.

Although $RALDH2^{high}$ $CD1c^+$ mDCs induced the expression of a higher level of $\alpha_4\beta_7$ integrin and reciprocally suppressed the expression of CLA on T cells in an RA-dependent manner, we could not observe the induction of CCR9 in the culture conditions we used. Spiegl et al. (26) also reported no CCR9 induction on human T cells by RA. Thus, the induction of CCR9 on human T cells may be more tightly regulated than that on mouse T cells.

VD_3 directly acts on T cells to induce skin-homing receptors (35). The present study showed that VD_3 induces T cells to express gut-homing receptors through inducing RA production by DCs. It appears to be difficult to reconcile these two phenomena. A possible scenario is that $CD1c^+$ mDCs are exposed to VD_3 in peripheral tissues, migrate into regional lymph nodes, and present RA to T cells. Indeed, tissue-resident cells such as epithelial cells and macrophages (36) express CYP27B1. As such, exposure of DCs to VD_3 may be spatially and chronologically separated from T cell stimulation by the DCs.

VD_3 and RA have been thought to reciprocally control immune responses in the skin and intestine (27). Thus, the induction of RALDH2 by VD_3 is counterintuitive. However, such dichotomy between VD_3 and RA are becoming blurred. On the one hand, VD_3 locally produced by epithelial cells and macrophages in various organs and lymphoid tissues (36) likely has an immunomodulatory effect in a paracrine manner (37). On the other hand, RA-producing DCs exist in extraintestinal as well as intestinal tissues and their corresponding draining lymph nodes (2). In addition, a wide variety of cells can produce GM-CSF. Thus, VD_3, RA, and GM-CSF are likely to have opportunities to collaborate and to stimulate $CD1c^+$ mDCs in various tissues, and such DCs may induce gut-homing T cells by producing RA in extraintestinal as well as intestinal compartments.

$RALDH2^{high}$ mDCs induced naive $CD4^+$ T cells to acquire the ability to produce Th2 cytokines in an RA-dependent and IL-4–independent manner. The apparently direct effect of RA on Th2 induction is consistent with our previous report with mice (38). It has been shown that RA derived from basophils also induces Th2 cells (26). Thus, RA derived from $CD1c^+$ mDCs as well as basophils may contribute to Th2 polarization.

It has been proposed that Th2-type allergic responses may constitute an important asset of the immune system to maintain tissue homeostasis by ameliorating inflammation and promoting tissue repair (39, 40). The present study suggests that locally produced VD_3 may induce RA-producing $CD1c^+$ mDCs that promote a "type 2" environment, thus contributing to maintaining tissue homeostasis. Inflammation caused by infections, exemplified by the stimulation of $CD1c^+$ mDCs with TLR ligands and TNF, may extinguish the Th2-inducing RA production, and turn on type 1 inflammation. Taken together with a recent report that VD_3-stimulated $CD1c^+$ blood mDCs produce IL-10 and induce Treg cells (41), $CD1c^+$ mDCs may represent a DC subset that maintains immune homeostasis. Furthermore, epidemiological studies have shown that a poor vitamin D status is associated with an increased risk of autoimmune diseases (37). Thus, it is intriguing to speculate that RA production by $CD1c^+$ mDCs stimulated with VD_3 contributes to prevention of autoimmune diseases in the steady state.

In conclusion, this study reveals a novel link between two key immunomodulatory vitamins (vitamin A and D) via a distinctive human DC subset, that is, $CD1c^+$ mDCs. This may constitute a previously unrecognized immune component for maintaining tissue homeostasis. Exploiting immunomodulatory activity of this component may lead to novel therapies or prevention of various autoimmune or inflammatory disorders.

Acknowledgments

We thank Keiko Fukunaga for excellent technical assistance.

Disclosures

The authors have no financial conflicts of interest.

References

1. Iwata, M., A. Hirakiyama, Y. Eshima, H. Kagechika, C. Kato, and S.-Y. Song. 2004. Retinoic acid imprints gut-homing specificity on T cells. *Immunity* 21: 527–538.
2. Guilliams, M., K. Crozat, S. Henri, S. Tamoutounour, P. Grenot, E. Devilard, B. de Bovis, L. Alexopoulou, M. Dalod, and B. Malissen. 2010. Skin-draining lymph nodes contain dermis-derived $CD103^-$ dendritic cells that constitutively produce retinoic acid and induce $Foxp3^+$ regulatory T cells. *Blood* 115: 1958–1968.
3. Coombes, J. L., K. R. R. Siddiqui, C. V. Arancibia-Cárcamo, J. Hall, C.-M. Sun, Y. Belkaid, and F. Powrie. 2007. A functionally specialized population of mu-

cosal CD103$^+$ DCs induces Foxp3$^+$ regulatory T cells via a TGF-β and retinoic acid-dependent mechanism. *J. Exp. Med.* 204: 1757–1764.
4. Yokota, A., H. Takeuchi, N. Maeda, Y. Ohoka, C. Kato, S.-Y. Song, and M. Iwata. 2009. GM-CSF and IL-4 synergistically trigger dendritic cells to acquire retinoic acid-producing capacity. *Int. Immunol.* 21: 361–377.
5. Villablanca, E. J., S. Wang, J. de Calisto, D. C. O. Gomes, M. A. Kane, J. L. Napoli, W. S. Blaner, H. Kagechika, R. Blomhoff, M. Rosemblatt, et al. 2011. MyD88 and retinoic acid signaling pathways interact to modulate gastrointestinal activities of dendritic cells. *Gastroenterology* 141: 176–185.
6. Feng, T., Y. Cong, H. Qin, E. N. Benveniste, and C. O. Elson. 2010. Generation of mucosal dendritic cells from bone marrow reveals a critical role of retinoic acid. *J. Immunol.* 185: 5915–5925.
7. Molenaar, R., M. Knippenberg, G. Goverse, B. J. Olivier, A. F. de Vos, T. O'Toole, and R. E. Mebius. 2011. Expression of retinaldehyde dehydrogenase enzymes in mucosal dendritic cells and gut-draining lymph node stromal cells is controlled by dietary vitamin A. *J. Immunol.* 186: 1934–1942.
8. Jaensson-Gyllenbäck, E., K. Kotarsky, F. Zapata, E. K. Persson, T. E. Gundersen, R. Blomhoff, and W. W. Agace. 2011. Bile retinoids imprint intestinal CD103$^+$ dendritic cells with the ability to generate gut-tropic T cells. *Mucosal Immunol.* 4: 438–447.
9. Elgueta, R., F. E. Sepulveda, F. Vilches, L. Vargas, J. R. Mora, M. R. Bono, and M. Rosemblatt. 2008. Imprinting of CCR9 on CD4 T cells requires IL-4 signaling on mesenteric lymph node dendritic cells. *J. Immunol.* 180: 6501–6507.
10. Uematsu, S., K. Fujimoto, M. H. Jang, B.-G. Yang, Y.-J. Jung, M. Nishiyama, S. Sato, T. Tsujimura, M. Yamamoto, Y. Yokota, et al. 2008. Regulation of humoral and cellular gut immunity by lamina propria dendritic cells expressing Toll-like receptor 5. *Nat. Immunol.* 9: 769–776.
11. Manicassamy, S., R. Ravindran, J. Deng, H. Oluoch, T. L. Denning, S. P. Kasturi, K. M. Rosenthal, B. D. Evavold, and B. Pulendran. 2009. Toll-like receptor 2-dependent induction of vitamin A-metabolizing enzymes in dendritic cells promotes T regulatory responses and inhibits autoimmunity. *Nat. Med.* 15: 401–409.
12. Wang, S., E. J. Villablanca, J. De Calisto, D. C. O. Gomes, D. D. Nguyen, E. Mizoguchi, J. C. Kagan, H.-C. Reinecker, N. Hacohen, C. Nagler, et al. 2011. MyD88-dependent TLR1/2 signals educate dendritic cells with gut-specific imprinting properties. *J. Immunol.* 187: 141–150.
13. Ziegler-Heitbrock, L., P. Ancuta, S. Crowe, M. Dalod, V. Grau, D. N. Hart, P. J. M. Leenen, Y.-J. Liu, G. MacPherson, G. J. Randolph, et al. 2010. Nomenclature of monocytes and dendritic cells in blood. *Blood* 116: e74–e80.
14. Jongbloed, S. L., A. J. Kassianos, K. J. McDonald, G. J. Clark, X. Ju, C. E. Angel, C.-J. J. Chen, P. R. Dunbar, R. B. Wadley, V. Jeet, et al. 2010. Human CD141$^+$ (BDCA-3)$^+$ dendritic cells (DCs) represent a unique myeloid DC subset that cross-presents necrotic cell antigens. *J. Exp. Med.* 207: 1247–1260.
15. Poulin, L. F., M. Salio, E. Griessinger, F. Anjos-Afonso, L. Craciun, J.-L. Chen, A. M. Keller, O. Joffre, S. Zelenay, E. Nye, et al. 2010. Characterization of human DNGR-1$^+$BDCA3$^+$ leukocytes as putative equivalents of mouse CD8α+ dendritic cells. *J. Exp. Med.* 207: 1261–1271.
16. Bachem, A., S. Güttler, E. Hartung, F. Ebstein, M. Schaefer, A. Tannert, A. Salama, K. Movassaghi, C. Opitz, H. W. Mages, et al. 2010. Superior antigen cross-presentation and XCR1 expression define human CD11c$^+$CD141$^+$ cells as homologues of mouse CD8$^+$ dendritic cells. *J. Exp. Med.* 207: 1273–1281.
17. Haniffa, M., A. Shin, V. Bigley, N. McGovern, P. Teo, P. See, P. S. Wasan, X. N. Wang, F. Malinarich, B. Malleret, et al. 2012. Human tissues contain CD141^{hi} cross-presenting dendritic cells with functional homology to mouse CD103$^+$ nonlymphoid dendritic cells. *Immunity* 37: 60–73.
18. Robbins, S. H., T. Walzer, D. Dembélé, C. Thibault, A. Defays, G. Bessou, H. Xu, E. Vivier, M. Sellars, P. Pierre, et al. 2008. Novel insights into the relationships between dendritic cell subsets in human and mouse revealed by genome-wide expression profiling. *Genome Biol.* 9: R17.
19. Stock, A., S. Booth, and V. Cerundolo. 2011. Prostaglandin E_2 suppresses the differentiation of retinoic acid-producing dendritic cells in mice and humans. *J. Exp. Med.* 208: 761–773.
20. Miyara, M., Y. Yoshioka, A. Kitoh, T. Shima, K. Wing, A. Niwa, C. Parizot, C. Taflin, T. Heike, D. Valeyre, et al. 2009. Functional delineation and differentiation dynamics of human CD4$^+$ T cells expressing the FoxP3 transcription factor. *Immunity* 30: 899–911.
21. Iyoda, T., S. Shimoyama, K. Liu, Y. Omatsu, Y. Akiyama, Y. Maeda, K. Takahara, R. M. Steinman, and K. Inaba. 2002. The CD8$^+$ dendritic cell subset selectively endocytoses dying cells in culture and in vivo. *J. Exp. Med.* 195: 1289–1302.
22. Ito, T., M. Inaba, K. Inaba, J. Toki, S. Sogo, T. Iguchi, Y. Adachi, K. Yamaguchi, R. Amakawa, J. Valladeau, et al. 1999. A CD1a$^+$/CD11c$^+$ subset of human blood dendritic cells is a direct precursor of Langerhans cells. *J. Immunol.* 163: 1409–1419.
23. Penna, G., and L. Adorini. 2000. 1α,25-Dihydroxyvitamin D3 inhibits differentiation, maturation, activation, and survival of dendritic cells leading to impaired alloreactive T cell activation. *J. Immunol.* 164: 2405–2411.
24. Piemonti, L., P. Monti, M. Sironi, P. Fraticelli, B. E. Leone, E. Dal Cin, P. Allavena, and V. Di Carlo. 2000. Vitamin D_3 affects differentiation, maturation, and function of human monocyte-derived dendritic cells. *J. Immunol.* 164: 4443–4451.
25. Penna, G., S. Amuchastegui, N. Giarratana, K. C. Daniel, M. Vulcano, S. Sozzani, and L. Adorini. 2007. 1,25-Dihydroxyvitamin D_3 selectively modulates tolerogenic properties in myeloid but not plasmacytoid dendritic cells. *J. Immunol.* 178: 145–153.
26. Spiegl, N., S. Didichenko, P. McCaffery, H. Langen, and C. A. Dahinden. 2008. Human basophils activated by mast cell-derived IL-3 express retinaldehyde dehydrogenase-II and produce the immunoregulatory mediator retinoic acid. *Blood* 112: 3762–3771.
27. Mora, J. R., M. Iwata, and U. H. von Andrian. 2008. Vitamin effects on the immune system: vitamins A and D take centre stage. *Nat. Rev. Immunol.* 8: 685–698.
28. Barone, F. C., E. A. Irving, A. M. Ray, J. C. Lee, S. Kassis, S. Kumar, A. M. Badger, R. F. White, M. J. McVey, J. J. Legos, et al. 2001. SB 239063, a second-generation p38 mitogen-activated protein kinase inhibitor, reduces brain injury and neurological deficits in cerebral focal ischemia. *J. Pharmacol. Exp. Ther.* 296: 312–321.
29. Davis, M. I., J. P. Hunt, S. Herrgard, P. Ciceri, L. M. Wodicka, G. Pallares, M. Hocker, D. K. Treiber, and P. P. Zarrinkar. 2011. Comprehensive analysis of kinase inhibitor selectivity. *Nat. Biotechnol.* 29: 1046–1051.
30. Mora, J. R., G. Cheng, D. Picarella, M. Briskin, N. Buchanan, and U. H. von Andrian. 2005. Reciprocal and dynamic control of CD8 T cell homing by dendritic cells from skin- and gut-associated lymphoid tissues. *J. Exp. Med.* 201: 303–316.
31. Szatmari, I., A. Pap, R. Rühl, J.-X. Ma, P. A. Illarionov, G. S. Besra, E. Rajnavolgyi, B. Dezso, and L. Nagy. 2006. PPARγ controls CD1d expression by turning on retinoic acid synthesis in developing human dendritic cells. *J. Exp. Med.* 203: 2351–2362.
32. Chang, S.-Y., H.-R. Cha, J.-H. Chang, H.-J. Ko, H. Yang, B. Malissen, M. Iwata, and M.-N. Kweon. 2010. Lack of retinoic acid leads to increased langerin-expressing dendritic cells in gut-associated lymphoid tissues. *Gastroenterology* 138: 1468–1478, e1–e6.
33. Bastie, J. N., N. Balitrand, F. Guidez, I. Guillemot, J. Larghero, C. Calabresse, C. Chomienne, and L. Delva. 2004. 1α,25-Dihydroxyvitamin D3 transrepresses retinoic acid transcriptional activity via vitamin D receptor in myeloid cells. *Mol. Endocrinol.* 18: 2685–2699.
34. Jaensson, E., H. Uronen-Hansson, O. Pabst, B. Eksteen, J. Tian, J. L. Coombes, P.-L. Berg, T. Davidsson, F. Powrie, B. Johansson-Lindbom, and W. W. Agace. 2008. Small intestinal CD103$^+$ dendritic cells display unique functional properties that are conserved between mice and humans. *J. Exp. Med.* 205: 2139–2149.
35. Sigmundsdottir, H., J. Pan, G. F. Debes, C. Alt, A. Habtezion, D. Soler, and E. C. Butcher. 2007. DCs metabolize sunlight-induced vitamin D3 to 'program' T cell attraction to the epidermal chemokine CCL27. *Nat. Immunol.* 8: 285–293.
36. Zehnder, D., R. Bland, M. C. Williams, R. W. McNinch, A. J. Howie, P. M. Stewart, and M. Hewison. 2001. Extrarenal expression of 25-hydroxyvitamin d(3)-1 α-hydroxylase. *J. Clin. Endocrinol. Metab.* 86: 888–894.
37. Hewison, M. 2012. An update on vitamin D and human immunity. *Clin. Endocrinol.* 76: 315–325.
38. Iwata, M., Y. Eshima, and H. Kagechika. 2003. Retinoic acids exert direct effects on T cells to suppress Th1 development and enhance Th2 development via retinoic acid receptors. *Int. Immunol.* 15: 1017–1025.
39. Allen, J. E., and T. A. Wynn. 2011. Evolution of Th2 immunity: a rapid repair response to tissue destructive pathogens. *PLoS Pathog.* 7: e1002003.
40. Palm, N. W., R. K. Rosenstein, and R. Medzhitov. 2012. Allergic host defences. *Nature* 484: 465–472.
41. Chu, C.-C., N. Ali, P. Karagiannis, P. Di Meglio, A. Skowera, L. Napolitano, G. Barinaga, K. Grys, E. Sharif-Paghaleh, S. N. Karagiannis, et al. 2012. Resident CD141 (BDCA3)$^+$ dendritic cells in human skin produce IL-10 and induce regulatory T cells that suppress skin inflammation. *J. Exp. Med.* 209: 935–945.

Journal of Medicinal Chemistry

Article

pubs.acs.org/jmc

Crystal Structures of Hereditary Vitamin D-Resistant Rickets-Associated Vitamin D Receptor Mutants R270L and W282R Bound to 1,25-Dihydroxyvitamin D_3 and Synthetic Ligands

Makoto Nakabayashi,*[,†,‡,∥] Yoshito Tsukahara,[†] Yukiko Iwasaki-Miyamoto,[‡] Mika Mihori-Shimazaki,[‡] Sachiko Yamada,*[,‡,∥] Satomi Inaba,[⊥] Masayuki Oda,[⊥] Masato Shimizu,[†,‡] Makoto Makishima,[∥] Hiroaki Tokiwa,[#] Teikichi Ikura,[§] and Nobutoshi Ito[§]

[†]Graduate School of Biomedical Science, [‡]Institute of Biomaterials and Bioengineering, and [§]Medical Research Institute, Tokyo Medical and Dental University, Bunkyo-ku, Tokyo 113-8510, Japan

[∥]Department of Biomedical Sciences, Nihon University School of Medicine, Itabashi-ku, Tokyo 173-8610, Japan

[⊥]Graduate School of Life and Environmental Sciences, Kyoto Prefectural University, Sakyo-ku, Kyoto 606-8522, Japan

[#]Department of Chemistry, Faculty of Science, Rikkyo University, Toshima-ku, Tokyo 171-8501, Japan

Supporting Information

ABSTRACT: The vitamin D receptor (VDR), a member of the nuclear receptor superfamily, functions as a ligand-dependent transcription factor for various genes. Hereditary vitamin D-resistant rickets (HVDRR), an autosomal recessive disease, is caused by mutations in the VDR. In particular, the missense mutations R274L and W286R in the ligand-binding domain of the VDR can severely reduce or even eliminate natural hormone responsiveness. Here, we report a crystal structure analysis of the R270L and W282R mutants of rat VDR (human R274L and W286R, respectively) in complex with the natural hormone and synthetic ligands. We also studied the folding properties of the mutant proteins by using circular dichroism spectra. Our study indicates that these mutations result in only local structural modifications. We discuss why these mutations disrupt the VDR function and provide clues to develop effective ligands for the treatment of HVDRR.

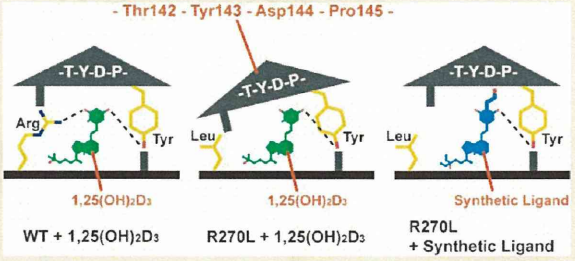

INTRODUCTION

Vitamin D_3 is acquired from dietary sources or via ultraviolet irradiation of 7-dehydrocholesterol in the epidermis. It is metabolized to its active hormonal form, 1,25-dihydroxyvitamin D_3 [$1,25(OH)_2D_3$] via the action of D_3 1α-hydrdoxylase (CYP27B1) expressed predominantly in the kidney.[1] $1,25(OH)_2D_3$ maintains calcium and phosphorus homeostasis in vertebrates[2] by directly binding to the vitamin D receptor (VDR)[3] in the intestine, kidney, and bone. This activity is regulated via feedback inhibition of parathyroid hormone production in the parathyroid glands. $1,25(OH)_2D_3$ is also produced locally in numerous cell types that express the VDR, notably skin, cells of the immune system, colon, pancreas, and vasculature.[4] The significance of the local extraosseous effects of $1,25(OH)_2D_3$ is not fully understood, but it appears that vitamin D, likely cooperating with other regulators, exerts immunoregulation, antimicrobial defense, xenobiotic detoxification, anticancer actions, control of insulin secretion, and, possibly, cardiovascular benefits.[5]

When vitamin D binds to the VDR, it changes its conformation to the active form and interacts with the 9-*cis*-retinoic acid receptor (RXR) forming a heterodimer.[6] The VDR/RXR heterodimer binds to vitamin D-responsive elements (VDRE) in the promoter region of target genes. The active conformation of the VDR forms a surface called the activation function 2 (AF-2) to which coactivator complexes are recruited, and this triggers complex events that lead to transactivation.[4]

Mutations in the VDR gene cause the genetic diseases hereditary vitamin D-resistant rickets (HVDRR, also known as vitamin D-dependent rickets, type II).[7] HVDRR, an autosomal recessive disorder, is characterized by early onset rickets, hypocalcemia, elevated serum $1,25(OH)_2D_3$ level, and secondary hyperparathyroidism. Mutations are found in both the DNA binding domain (DBD) and ligand binding domain (LBD) of the VDR. One major therapeutic approach to HVDRR is the intravenous injection of calcium;[7b] however, this treatment must be continued for a long period and fails to improve patients' quality-of-life. Therefore, other therapeutic options are needed. For example, small compounds might

Received: April 14, 2013
Published: August 14, 2013

   dx.doi.org/10.1021/jm400537h | *J. Med. Chem.* 2013, 56, 6745−6760

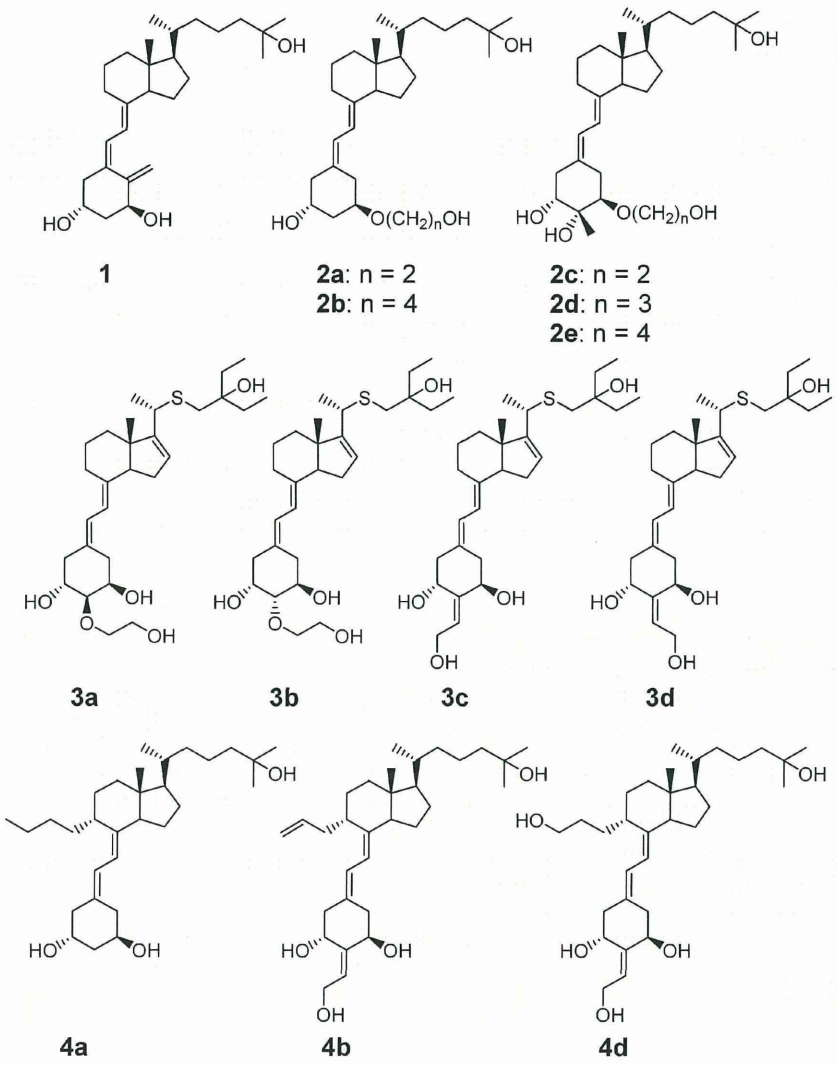

Figure 1. Structures of the vitamin D analogues discussed in this article.

rescue the functions disrupted by the missense mutations in the VDR-LBD.

Fifteen missense mutations have been identified in the LBD[7b] that reduce or abolish VDR functions, such as ligand binding and ligand-dependent transactivation. So far, only the crystal structure of the HVDRR H305Q mutant has been reported.[8] The H305Q mutation causes a 10-fold reduction in $1,25(OH)_2D_3$-dependent transactivation, and patients with this mutation can be treated with the natural hormone. The missense mutation R274L,[9] however, causes a >1000-fold reduction in responsiveness to the natural hormone. Patients with this mutation are hardly responsive to treatment with $1,25(OH)_2D_3$. Another severe mutation is W286R.[10] Patients with this mutation never respond to the natural hormone.

Here, we present the crystal structures of rat (r) VDR-LBD R270L and W282R mutants, which correspond to the human (h) R274L and W286R VDR mutants, respectively. We also designed and synthesized several ligands (**2a–e**, **3a–d**, and **4a–e**) (Figure 1) for use with these mutants. On the basis of these crystal structures and results of in vitro biological assays with ligands (**2a–e**, **3a–d** and **4a–e**), we discuss how these mutations disrupt the VDR function. Our data also provide clues for the design of novel therapeutic compounds for the treatment of HVDRR patients. Thermal unfolding experiments and CD spectral analysis also provided data that could not be obtained from the X-ray analysis alone to characterize these mutants.

RESULTS

Crystal Structures. We crystallized the rat VDR-LBD with a deletion mutation (rVDR-LBD 116–423, Δ165–211) in the long loop between helices H2 and H3[11] because it readily provided high quality crystals even with the point mutations. Human and rat VDRs share 89.5% identity overall and are 97.2% identical within the ligand-binding pocket (LBP). Therefore, crystal structures of rVDR-LBD mutants also provide important structural information about hVDR-LBD mutants. From this point in this article, rVDR-LBD (Δ165–211) will be referred to as WT, and its substitution mutants will be referred to as R270L and W282R, respectively.

The crystals of WT, R270L, and W282R were grown in the presence of the natural hormone (**1**) or one of the ligands

dx.doi.org/10.1021/jm400537h | J. Med. Chem. 2013, 56, 6745–6760

designed for the mutants (**3c** and **3d** for R270L, **4a** and **4b** for W282R; Figure 1) and with a peptide containing the LXXLL motif derived from the coactivator DRIP205 (MED1).[12] This peptide, which is essential for crystallizations, not only stabilizes the crystals by binding to the surface between the termini of the helices H3 and H12, known as the coactivator recognition surface (the AF-2 surface), but also participates in crystal packing (Figure S1, Supporting Information).

All of the crystals belonged to the same space group C2 as other rVDR complexes do.[11,13] The R270L complexes with ligands **1**, **3c**, and **3d** were refined to resolutions of 1.70, 1.90, and 2.11 Å (PDB ID: 3VT3, 3VT4, and 3VT5, respectively). The WT complex with ligand **3c** was refined to a resolution of 2.30 Å (PDB ID: 3VT6). The W282R complexes with ligands **1**, **4a**, and **4b** were refined to resolutions of 1.65, 2.10, and 2.35 Å (PDB ID: 3VT7, 3VT8, and 3VT9, respectively). Summaries of data collection and refinement statistics are shown in Tables S1, S2, and S3 (Supporting Information).

The overall folds of the VDR-LBDs in these complexes were fundamentally identical to those of the known h- and rVDR-LBD complexes with the natural hormone,[11a,14] as well as its agonistic[13c,15] and antagonistic analogues.[11b,13a,b,d] All seven complexes adopted the canonical active conformation of the VDR-LBD, and the coactivator peptide bound to the AF-2 surface. The root-mean-square deviations (rmsd) of the equivalent Cα atoms of the mutants (R270L and W282R) complexed with 1,25$(OH)_2D_3$ and the synthetic ligands (**3c**, **3d**, **4a**, and **4b**) from the corresponding WT complex (PDB ID: 2ZLC) were 0.15 to 0.30 Å. For comparison, we used rVDR-LBD (2ZLC) reported by us[16] but not that (1RK3) reported by Vanhooke's group[11a] because the conditions we used to prepare the crystals were nearly identical to those used for 2ZLC. The difference in the crystallization conditions used caused some changes in the loop region structures (rmsd, 0.4–0.9 Å). In calculating Cα rmsds, we eliminated the terminal atoms that had large rmsds values of >1.00.

R270L Complexed with the Natural Hormone 1,25-$(OH)_2D_3$. We successfully crystallized R270L complexed with 1,25$(OH)_2D_3$ in its active ternary complex as evidenced by the corresponding density clearly seen in the $2F_{obs} - F_{calc}$ map (Figure S2, Supporting Information). The Cα structure was nearly identical to that of WT (2ZLC), as indicated by the total rmsd (0.15 Å). The Cα positions shifted slightly near the mutation, Leu269 (0.45 Å) and Met268 (0.30 Å). Two water molecules are found in the space created by the mutation of arginine to leucine (Figure 2A); one of these water molecules forms a hydrogen bond with the 1α-OH group, and the other forms a hydrogen bond with the main chain carbonyl group of Thr142. These interactions, however, must be weak because the human R274L mutant showed a greater than 1000-fold reduction in transcriptional responsiveness to the natural hormone.[9] In the WT, Arg270 formed direct hydrogen bonds with the 1α-OH group and the main chain carbonyl of Thr142. These direct interactions might be important to keep the conformation of the loop 1–2 and for the function of the VDR. Ligand recognition by the mutant, otherwise, is very similar to that of the WT, that is, 1,25$(OH)_2D_3$ (**1**) is anchored by five hydrogen bonds.

R270L in Complex with Ligands 3c and 3d. Ligands **3c** and **3d** are super agonists for wild-type hVDR.[16] They were also good agonists for R274L hVDR, being 130 and 40 times, respectively, more potent than **1** (see below). The complexes of R270L with **3c** and **3d** adopt the same active conformation as

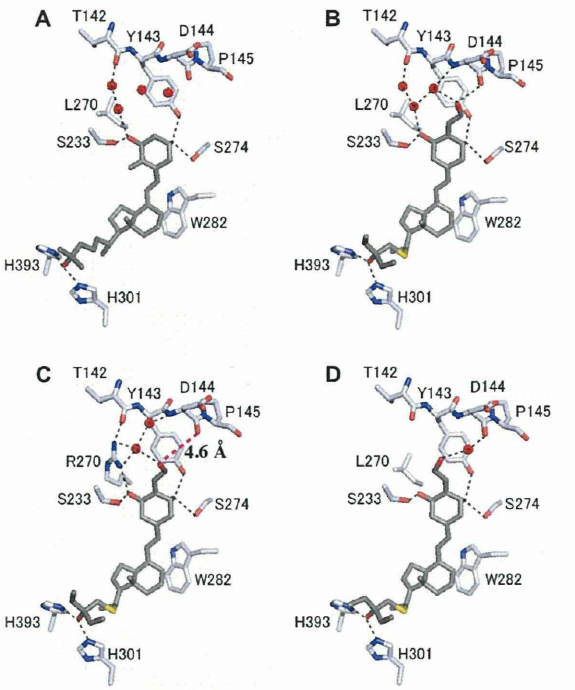

Figure 2. Hydrogen-bonding interactions in the complexes of R270L. (A) R270L with **1**, (B) R270L with **3c**, (C) WT with **3c**, and (D) R270L with **3d**. Black dotted lines show hydrogen bonds. Ligands (dark gray, carbon; red, oxygen; and yellow, sulfur) and protein residues (white, carbon; red, oxygen; and blue, nitrogen) are shown as sticks and water molecules as red balls. The magenta dotted line in C shows the distance between the terminal hydroxyl group of **3c** and the main chain carbonyl group of Asp144.

that of the WT. The Cα rmsds of R270L complexed with **3c** and **3d** from WT (2ZLC) were 0.23 and 0.19 Å, respectively.

In the complex of R270L with **3c**, the terminal hydroxyl group of the substituent at C(2) directly interacts with the main chain carbonyl group of Asp144 (Figure 2B). This interaction replaced the lost direct interactions among the 1α-OH group of the ligand, Arg270, and Thr142 and explain why **3c** was 130 times more active than **1** for hR274L. The defective interaction with L270 made the ligand slightly move to Asp144 to form the hydrogen bond. In the complex with WT (Figure 2C), the terminal hydroxyl group of **3c** was 4.6 Å away from the carbonyl group of Asp144. Compound **3c** also interacted with Thr142 via two water molecules (Figure 2B). Because of these interactions, the Cα positional shifts of Thr142, Asp144, and Pro145 from those of the WT/1,25$(OH)_2D_3$ complex were somewhat large at 0.40, 0.55, and 0.63 Å, respectively. These changes might affect the conformation of Gln273 (positional shift, 0.48 Å) and Ser274 (0.48 Å) in the H5. Other than this difference, **3c**'s interaction with R270L was essentially identical to that with WT.

In the complex with R270L, **3d** does not directly hydrogen bond with Asp144, but it does hydrogen bond with a water molecule that, in turn, interacted with Asp144 (Figure 2D). This difference explains the difference in the activity of **3d** compared with **3c**.

W282R with Several Ligands. Trp286 in the hVDR-LBD (Trp282 in rVDR-LBD) interacts strongly with the vitamin D ligand.[11a,14] The interactions occur at its 2-, 3a-, 4-, and 7a-

dx.doi.org/10.1021/jm400537h | J. Med. Chem. 2013, 56, 6745–6760

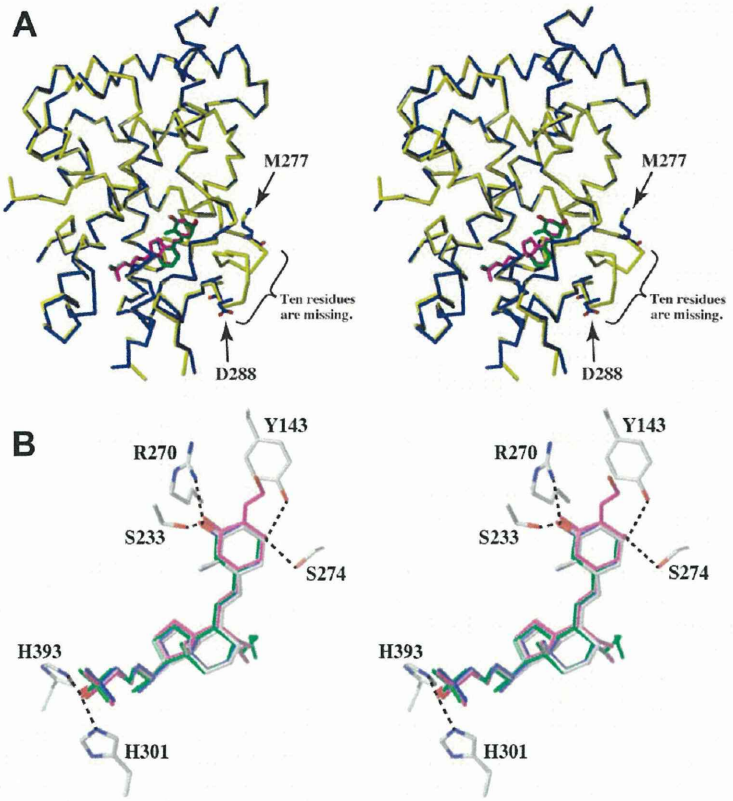

Figure 3. Overlays of the crystal structures of W282R and WT (stereoviews). (A) Overlay of the Cα structures of W282R and WT in complex with $1,25(OH)_2D_3$ (WT, yellow protein with green ligand; W282R, blue protein with magenta ligand). The W282R structure lacks 10 residues from Asp278 to Gln287. (B) Overlay of the ligands in WT (2ZLC) (atom type) and in W282R (**1**, **4a**, and **4b**; blue, green, and magenta, respectively) and the hydrogen-bonding residues in 2ZLC. The dotted lines show hydrogen bonds.

positions with the 6-, 8-, and 9-positions of the ligand over distances of less than 4 Å (Figure S3A, Supporting Information). The Trp286 also interacts with Phe279, Gln317, Tyr295, Ser275, Ser278, Leu313, and Ile314. As a result, its mutation to Arg abolishes the activity of the VDR mutant.[10]

We succeessfully crystallized ternary complexes of the W282R mutant with the natural hormone and two synthetic ligands (**4a** and **4b**), and the coactivator-derived peptide. The 9α-substituted ligands (**4a** and **4b**) were designed on the basis of the model of the mutants. The substituent at the 9α-position was directed toward Trp282 and expected to occupy the space yielded by the Trp to Arg mutation (Figures S3B and S4C, Supporting Information).

W282R in Complex with the Natural Hormone. The crystal structure of W282R in complex with the natural hormone was determined as the canonical active conformation (Figure 3A). Surprisingly, a group of residues neighboring of Arg282 were not visible in the electron density map of the mutant complex with the natural hormone (Figures 4A and B), suggesting that these residues were highly disordered. We did not observe any interpretable density in the W282R structure for 10 residues between Asp278 and Gln287 (Figure 4A). This disorder at the β-strand part affected the conformation of the beginning of loop 1–2, from Pro145 to Ala148 (positional shift, 0.35–0.79 Å). Yet, despite such a drastic disorder in the secondary structure, the overall folds of the mutant remain nearly identical to those of the WT (rmsd 0.27 Å) (Figure 3A). We assume that the coactivator peptide trapped the active conformation of the mutant by binding to the AF-2 surface, which formed temporally when the mutant bound the ligand. Thus, the seemingly minor conformation of W282R in biological solutions was crystallized out under our crystallization conditions. Surprisingly, the ligand forms normal hydrogen bonds via its three hydroxyl groups (Figure 3B).

W282R with 9-Substitued Vitamin D Analogues (4a and 4b). The complexes of W282R with **4a** and **4b** exhibited similar disorder near the antiparallel β-sheet; the seven residues from Asp279 to Gly285 were not visible. In addition, the ligands themselves had high temperature factors at the terminal of the 9-substituent groups. For example, in the complex of W282R with **4a** or **4b**, the terminal atom of the 9-substituent had an especially high value of more than 45 Å^2 (Figures S3C and D, Supporting Information). Thus, the terminal atoms of the 9-substituents cannot be stabilized via interactions to receptor residues that are also disordered. However, both **4a** and **4b** form normal hydrogen bonds via their three hydroxyl groups (Figure 3B).

Ligand Additive Effects and Thermal Unfolding of rVDR-LBD Mutants Observed by Far-UV CD Spectra. To examine the thermal stability of the R270L and W282R mutants compared with WT, we monitored heat-induced unfolding transition experiments using CD spectra.[17] Equilibrium CD spectra were obtained in the far-UV regions at pH 7.0. The far-UV spectrum of a solution of ligand-free WT at 20 °C exhibited the typical spectrum of an α-helical structure, and

dx.doi.org/10.1021/jm400537h | J. Med. Chem. 2013, 56, 6745–6760

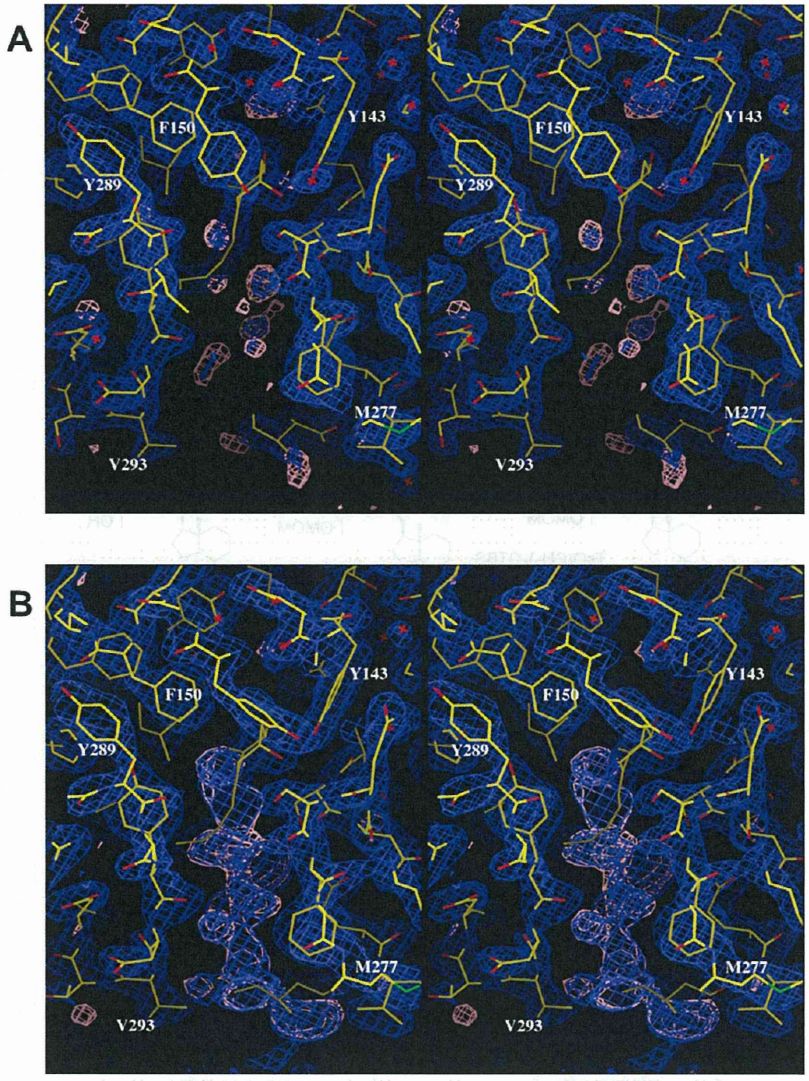

Figure 4. Electron density maps of W282R and WT complexes. (A) Electron density map of W282R/1,25$(OH)_2D_3$ around the β-sheet region (stereo view). (B) Electron density map of WT/1,25$(OH)_2D_3$ (PDB ID: 2ZLC) in the same region and orientation as that described above (stereo view). The $2F_{obs} - F_{calc}$ map (1.5 σ) is shown in blue, and the $F_{obs} - F_{calc}$ map (3 σ) is shown in pink. Notice that electron density around R282 (from Asp278 to Gln287) is missing in A but not in B.

the addition of the natural hormone confirmed this α-helical type spectrum[18] (Figure S5A, Supporting Information). R270L and W282R showed similar α-helical spectra to that of WT including the ligand-additive effect (Figures S5B and C, Supporting Information).

However, the three proteins WT, R270L, and W282R showed remarkable differences in their thermal stability. Figure S5D, E, and F (Supporting Information) shows the equilibrium transition curves at 222 nm of WT, R270L, and W282R, respectively, with and without the natural hormone. In the ligand-free solutions, the transition temperature (T_m) of WT was the highest (47.8 °C), whereas those of R270L and W282R were similarly lower (44.1 and 44.8 °C, respectively). In the presence of the natural ligand, the differences in the T_m values were more distinct. Ligand binding caused the T_m of WT to rise by 8.4 °C, whereas the T_m of R270L and W282R rose by only 2.5 and 0.1 °C, respectively. These results indicate that the ligand significantly stabilizes the WT but only weakly stabilizes R270L and has no stabilization effect on W282R. These results are consistent with the ligand binding behavior of the three proteins.

Synthesis of Agonists for Mutants R274L and W286R.

Agonist for R274L. Several studies have been reported to create specific agonist for mutants implicated in HVDRR. Swann et al.[19] reported that nonsecosteroidal ligands with a bisphenol scaffold showed potent transactivation for R274L. Kittaka et al. reported that vitamin D_3 analogues modified at the 1α-, 1β-, or 2α-position on the A-ring of vitamin D_3 improved the vitamin D action on the R274A and R274L mutants.[20]

We also designed and synthesized candidates of **2a–2e** and **3a–d** for hR274L (rR270L) (Figure 1). These candidates are 19-norvitamin D_3 analogues modified at the 1α-position (**2a** and **2b**), 1α- and 2-positions (**2c–2e**), and the side chain and 2-position (**3a–3d**).[16] Computer-aided molecular modeling

dx.doi.org/10.1021/jm400537h | J. Med. Chem. 2013, 56, 6745–6760

Scheme 1. Synthesis of Ligands 2a and 2b

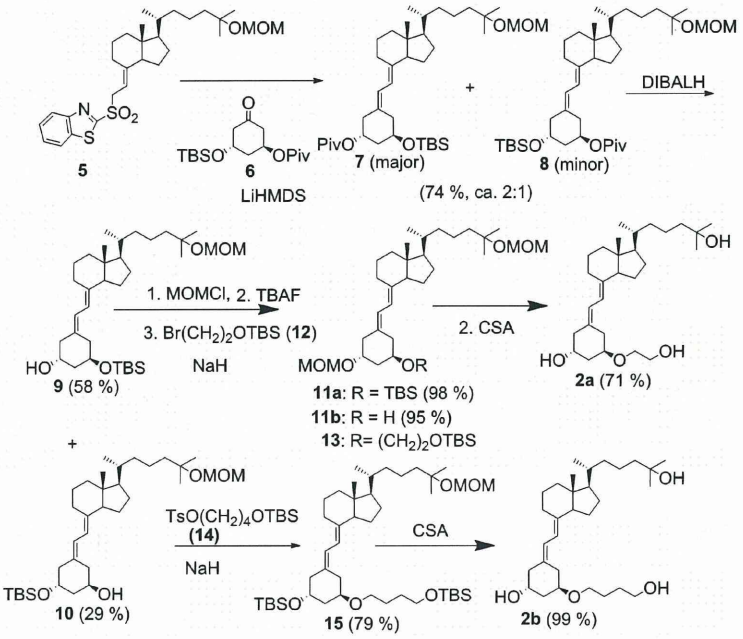

Scheme 2. Synthesis of Ligands 2c to 2e

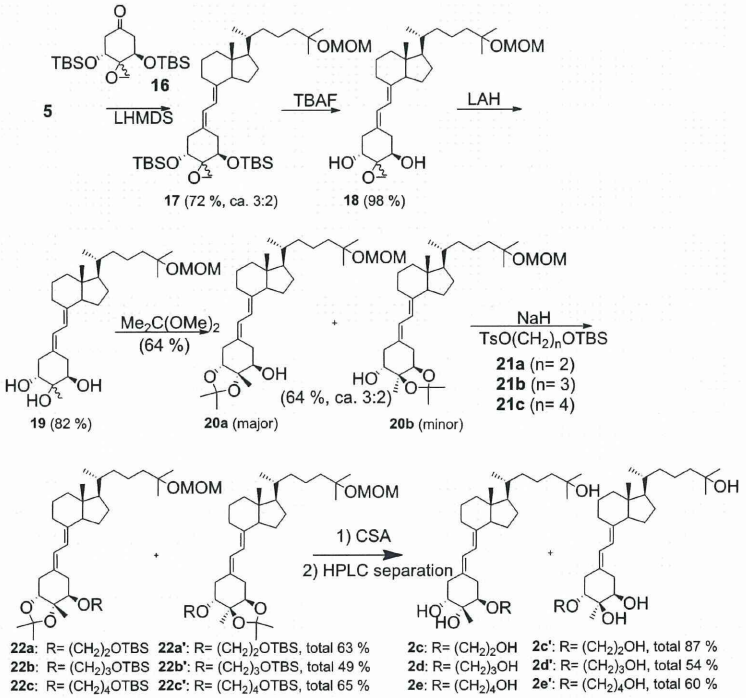

(Sybyl, Tripos) was used to design these ligands. The long substituent at the 1α-position was designed to fill the space newly generated by the Arg to Leu mutation (Figure S4A, Supporting Information). The 2α-methyl group of **2c**–**2e** was expected to interact with the hydrophobic residue above the A-ring and the 2β-hydroxyl group with the polar environment below the A ring.

The synthetic scheme of **2a** and **2b** is shown in Scheme 1. Julia-Kocienski reagent **5**[21] was coupled with A-ring fragment **6**, in which 1α- and 3β-hydroxyl groups were distinguished by protecting groups, to give 19-norvitamin D **7** and **8** as a 2:1 mixture (74%). After the pivaloyl group was removed (DIBALH), the free hydroxyl group of **9** was protected with the methoxymethyl (MOM) group (98%), and the *t*-butyldimethylsilyl (TBS) group was deprotected (95%) and

dx.doi.org/10.1021/jm400537h | J. Med. Chem. 2013, 56, 6745–6760

Scheme 3. Synthesis of Ligands 4a–4e

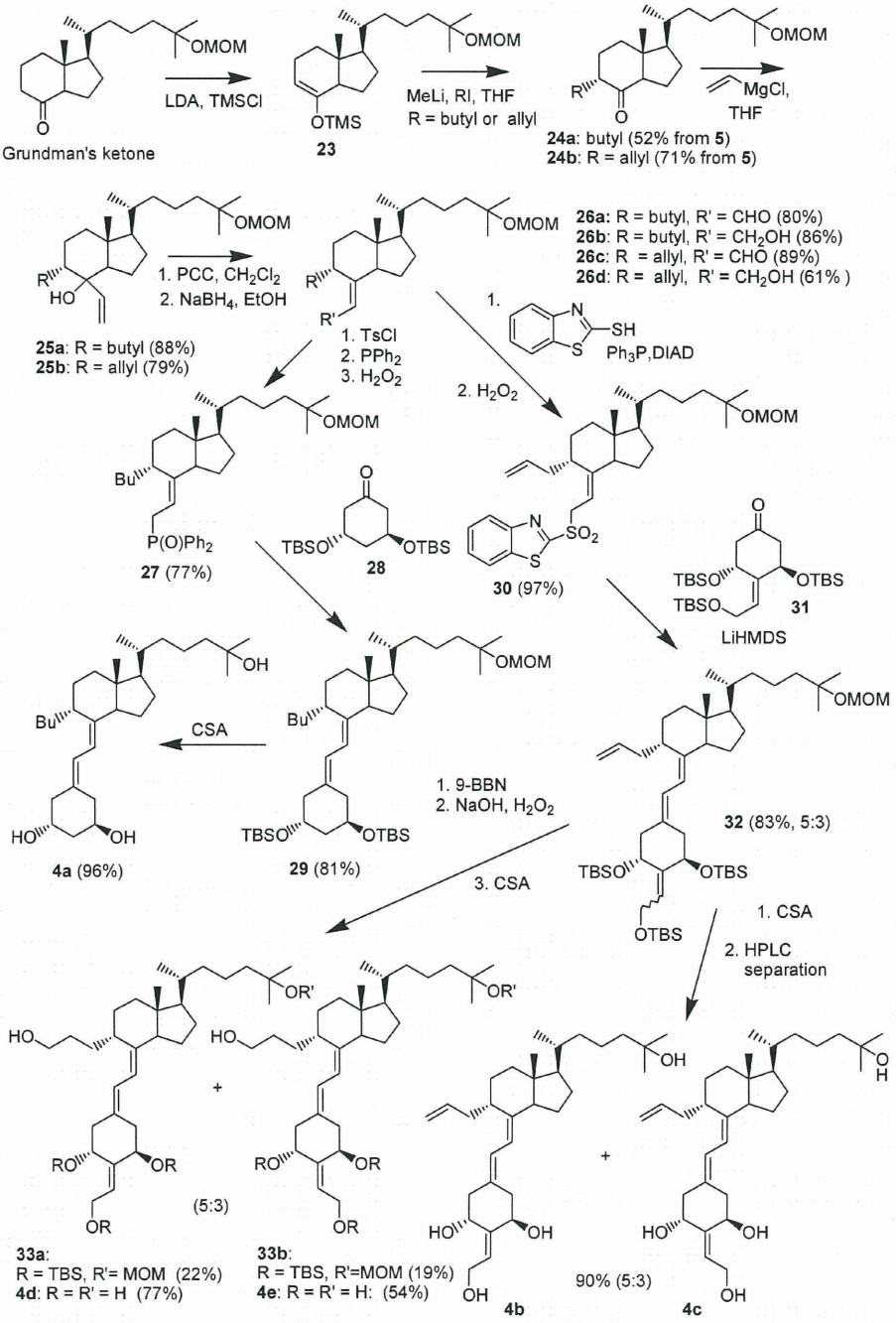

then treated with bromide **12** to give **13** (23%), the protecting groups of which were removed with camphor sulfonic acid (CSA) in MeOH to give 1α-hydroxyethoxy compound **2a** (71%). The hydroxy group of **10** was treated with tosylate **14** to give **15** (79%), the protecting groups of which were removed with CSA to give **2b** (99%).

The analogues **2c–e** were synthesized from **5** (Scheme 2). Compound **5** was treated with A-ring fragment **16** (72%), the TBS group was removed (98%), and the epoxide group was reduced with LAH to give triol **19** as an epimeric mixture at C(2) (82%). The *cis*-vicinal hydroxyl group of **19** was protected with 2,2-dimethoxypropane to give a 3:2 mixture of 2,3 (**20a**)- and 1,2-ketals (**20b**) (64%), and the remaining hydroxyl group was treated with tosylates **21a**, **21b**, and **21c** to give **22a**, **22b**, and **22c** (63%, 49%, and 65%), respectively. The protecting groups were removed with CSA, and then the products were separated by HPLC to give **2c**, **2d**, and **2e** and their regioisomers (total 87%, 54%, and 60%, respectively). The synthesis of **3a–d** was reported previously.[16]

Agonist for W286R. Using models of the W282R mutant, we hypothesized that a larger butyl group added to replace the 9α-hydrogen of vitamin D (Figure S3B, Supporting Information)

dx.doi.org/10.1021/jm400537h | J. Med. Chem. 2013, 56, 6745–6760